Multifractality at the Quantum Hall Transition: Beyond the Parabolic Paradigm

F. Evers,[1,2] A. Mildenberger,[3] and A. D. Mirlin[1,2,*]

[1]*Institut für Nanotechnologie, Forschungszentrum Karlsruhe, D-76021 Karlsruhe, Germany*
[2]*Institut für Theorie der Kondensierten Materie, Universität Karlsruhe, D-76128 Karlsruhe, Germany*
[3]*Fakultät für Physik, Universität Karlsruhe, D-76128 Karlsruhe, Germany*

(Received 28 April 2008; published 8 September 2008)

We present an ultrahigh-precision numerical study of the spectrum of multifractal exponents Δ_q characterizing anomalous scaling of wave function moments $\langle|\psi|^{2q}\rangle$ at the quantum Hall transition. The result reads $\Delta_q = 2q(1-q)[b_0 + b_1(q-1/2)^2 + \cdots]$, with $b_0 = 0.1291 \pm 0.0002$ and $b_1 = 0.0029 \pm 0.0003$. The central finding is that the spectrum is not exactly parabolic: $b_1 \neq 0$. This rules out a class of theories of the Wess-Zumino-Witten type proposed recently as possible conformal field theories of the quantum Hall critical point.

DOI: 10.1103/PhysRevLett.101.116803 PACS numbers: 73.43.−f, 05.45.Df, 71.30.+h, 72.15.Rn

Introduction.—The quantum Hall effect is a famous macroscopic quantum phenomenon [1,2] whose discovery gave rise to one of the most active research areas in condensed matter physics of past three decades. The plateaus with quantized values of the Hall conductivity are separated by quantum Hall transitions, which represent a celebrated example of a quantum critical point in a disordered electronic system (for a recent review, see Ref. [3]). Identification of the critical field theory of the integer quantum Hall transition remains a major unsolved problem of condensed matter physics.

One of the key characteristics of the quantum Hall transition point is the multifractality spectrum governing fluctuations of amplitudes of critical wave functions. Specifically, the moments of wave functions scale with system size L, with a set of anomalous exponents Δ_q,

$$\langle|\psi(\mathbf{r})|^{2q}\rangle/\langle|\psi(\mathbf{r})|^2\rangle^q \sim L^{-\Delta_q}. \tag{1}$$

(The angular brackets denote the ensemble averaging.) Equivalently, one often characterizes multifractality by a closely related set of exponents $\tau_q \equiv d(q-1) + \Delta_q$ or by its Legendre transform $f(\alpha)$ ("singularity spectrum") defined via $\alpha_q = \tau_q'$, $f(\alpha_q) = q\alpha_q - \tau_q$. Here d is the system dimensionality (while $d = 2$ for the present case of the quantum Hall transition, we find it useful to keep it as d in formulas below), and the prime denotes the q derivative.

Zirnbauer [4] and Tsvelik [5,6] conjectured that the conformal theory of the quantum Hall critical point is of the Wess-Zumino-Witten type. These proposals imply [7] that the spectrum Δ_q is parabolic, i.e., that γ_q defined according to

$$\Delta_q = \gamma_q q(1-q) \tag{2}$$

is in fact q-independent [8]: $\gamma_q = \gamma$. An accurate numerical analysis of the multifractal spectrum plays, therefore, a crucial role for identification of the critical theory.

A high-accuracy evaluation of the multifractality spectrum was carried out in our earlier work [9]. For this purpose, we modeled systems of a much larger size than in preceding works and performed averaging over a large ensemble of wave functions, as well as a thorough analysis of finite-size effects. It was found that the spectrum is close-to-parabolic [$\Delta_q \simeq \gamma q(1-q)$, with $\gamma = 0.262 \pm 0.003$], thus showing that, if deviations from parabolicity are present, they are rather small (of the order of 1%). While the data of Ref. [9] were showing some indications for such deviations, they were smaller than the numerical uncertainties. The latter originate from statistical noise (limited size of the data set) and from finite-size effects affecting the scaling relation (1) which is used to extract Δ_q.

The goal of the present Letter is to determine the Δ_q spectrum with an ultrahigh precision and to give an ultimate answer on the question, "Is the multifractality spectrum of the quantum Hall transition strictly parabolic?" For this purpose, we improve upon the earlier numerical analysis in two different ways. First, we utilize a statistical ensemble that contains approximately 10 times more samples than the one used before [9]. Second, we employ a recently discovered [10] "reciprocity relation"

$$\Delta_q = \Delta_{1-q} \tag{3}$$

for a better control of finite-size corrections.

Relation (3) implies a symmetry of the Δ_q spectrum around the point $q = 1/2$. Consequently, an expansion of γ_q about this point has a form

$$\gamma_q/d = b_0 + b_1(q-1/2)^2 + b_2(q-1/2)^4 \ldots. \tag{4}$$

To verify or to exclude parabolicity of Δ_q, the prefactor b_1 of the quadratic term (and possibly those of higher-order terms) in Eq. (4) should be determined numerically. This is the purpose of the present work. We will provide numerical evidence that the corrections to parabolicity do not vanish. Specifically, we obtain $b_0 = 0.1291 \pm 0.0002$ and $b_1 = 0.0029 \pm 0.0003$, the nonzero b_1 implying that the para-

bolicity is not exact. The corresponding value of α_0 [position of the apex of the singularity spectrum $f(\alpha)$] is $\alpha_0 = d + \gamma_0 = 2.2596 \pm 0.0004$.

Method.—In order to find the critical eigenstates, we employ the same numerical strategy that has been developed before [9]. We determine the lattice time evolution operator U for the Chalker-Coddington network model [11,12] with periodic boundary conditions and $N = 2L^d$ nodes. For each realization of disorder, eight eigenstates $\psi_\alpha(\mathbf{r})$ with eigenvalues closest to unity are found with a standard sparse matrix package [13–15] from exact diagonalization of U. (In the Chalker-Coddington model, the spatial coordinate $\mathbf{r}$ labels the links of the network.) We study systems with $L = 16, 32, 64, \ldots, 1024$ with $\sim 10^6$ samples for the smallest sizes and $\sim 10^4$ for the largest ones. The statistical analysis proceeds via calculating the average inverse participation ratios

$$P_q = N\langle|\psi^2|^q\rangle. \tag{5}$$

The symbol $\langle\ldots\rangle$ in Eq. (5) indicates the combined averaging of the amplitude moments $|\psi_\alpha(\mathbf{r})|^{2q}$ over (i) all spatial points (links) $\mathbf{r}$ in the sample, (ii) the energy window considered (here always eight eigenstates ψ_α per sample), and (iii) the statistical ensemble of samples with different microscopic realizations of disorder. The average inverse participation ratios P_q thus obtained obey the scaling law

$$P_q = c_q(N)N^{-(q-1)-\Delta_q/d}. \tag{6}$$

The coefficients c_q become independent of N in the limit $N \to \infty$.

As an alternative approach, we consider the ratio

$$L_q = \frac{\langle|\psi^2|^q \ln|\psi|^2\rangle}{\langle|\psi^2|^q\rangle} \equiv (\ln P_q)' = -\frac{\alpha_q}{d}\ln N + (\ln c_q)', \tag{7}$$

whose scaling yields the exponent $\alpha_q = \Delta_q' + d$. In this way, the exponent α_q is studied directly, i.e., without invoking a numerical differentiation which can significantly increase the error bars. In analogy with Eq. (4), we can expand Δ_q' around $q = 1/2$:

$$\Delta_q' = (1-2q)\tilde{\gamma}_q, \qquad \frac{\tilde{\gamma}_q}{d} = a_0 + a_1\left(q - \frac{1}{2}\right)^2 + \cdots. \tag{8}$$

The coefficients of both expansions are related via $a_0 = b_0 - b_1/4$, $a_1 = 2b_1 - b_2/2, \ldots$.

The averages entering Eqs. (5) and (7) are readily obtained numerically. It is beneficial to perform the scaling analysis of the ratio (7) in addition to that of Eq. (5) for several reasons. First, the curvature of Δ_q is more clearly seen in the q derivative Δ_q'. Second, the finite-size corrections are different in the cases of Eqs. (5) and (7), so that an agreement between the obtained exponents provides an additional confirmation of the validity of the $N \to \infty$ extrapolation procedure. Also, the relation $a_1 = 2b_1 - b_2/2$ allows one to extract the coefficient b_2 of the quartic term in Eq. (4) out of parabolic fits for γ_q and $\tilde{\gamma}_q$.

Numerical results.—We begin the analysis of our numerical results by verifying the reciprocity relation (3). To this end, we consider the ratio

$$r_q = N^{2q-1}\frac{P_q}{P_{1-q}} = N^{(\Delta_{1-q}-\Delta_q)/d}\frac{c_q(N)}{c_{1-q}(N)}. \tag{9}$$

The reciprocity relation (3) implies that the leading powers should cancel, so that r_q exhibits only subleading corrections in $1/N$. The log-linear plot (Fig. 1, upper row) shows that r_q saturates in the large N limit with a very well defined asymptotic value. Thus, we confirm reciprocity for the exponent spectrum of the integer quantum Hall effect, as expected [10]. Since the exponent relation must hold only in the asymptotic regime, we can draw another conclusion which is important for the subsequent analysis: The observed saturation of r_q provides evidence that our numerically accessible sample sizes are indeed large enough in order to be able to study the true asymptotics.

Similar to r_q, we consider the logarithmic derivative

$$s_q \equiv (\ln r_q)' = \frac{2d - \alpha_q - \alpha_{1-q}}{d}\ln N + (\ln c_q c_{1-q})', \tag{10}$$

which also saturates well inside the numerical window; see Fig. 1, lower row. Thus, the true asymptotics of α_q may be studied by means of Eq. (7) with available system sizes, too.

Having gone through important prerequisites, we now turn to the analysis of the main data. In order to determine a

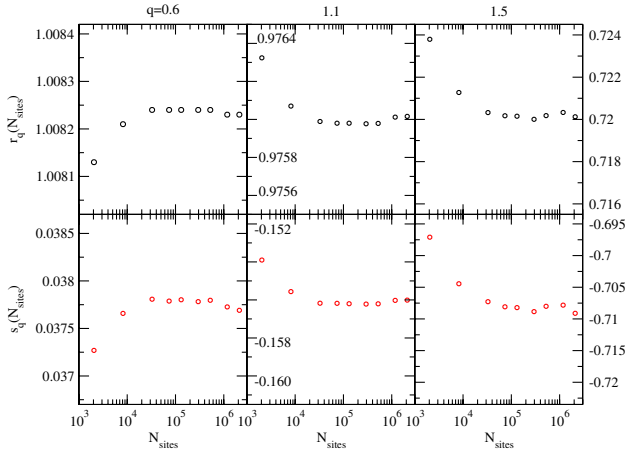

FIG. 1 (color online). Upper row: Ratio r_q of inverse participation numbers P_q and P_{1-q} [Eq. (9)] at $q = 0.6$, 1, and 1.5 (from left to right). The flat asymptotics indicates the validity of the reciprocity relation $\Delta_q = \Delta_{1-q}$. Small deviations from the constant behavior at the largest system sizes are due to residual statistical noise. Lower row: Analogous plots for the logarithmic derivative $s_q = (\ln r_q)'$ defined in Eq. (10).

set of relatively small exponents Δ_q to an accuracy considerably better than 1%, we have developed the following procedure. In each panel of Fig. 2, we plot for fixed q a family of curves labeled by a parameter δ:

$$F_q(N) = P_q N^{q-1+\delta(1-q)q}. \tag{11}$$

For the particular family member for which $F_q(N)$ becomes independent of N in the limit of large N, we can conclude that $\delta = \gamma_q/d$. From such a procedure, we extract the function γ_q without having to resort to any (multiparameter) fitting procedure. Similarly, by studying yet another family of curves

$$\tilde{F}_q(N) = L_q + \ln N[1 + (1 - 2q)\tilde{\delta}], \tag{12}$$

we have direct access also to the function $\tilde{\gamma}_q$ [see Eq. (8)] without the need for numerical differentiation.

The functions γ_q and $\tilde{\gamma}_q$ representing the main result of this Letter are displayed in Fig. 3. Also shown is $\Delta_q/q(1-q)$ as derived from the earlier evaluation of the exponents [9] (the size of corresponding error bars is indicated by dotted lines). Figure 3 clearly shows that the curvature in γ_q, which apparently has already left its trace in the earlier data, now fully reveals itself thanks to the reduced error bars. Even more pronounced is the resulting structure in the derivative $\tilde{\gamma}_q$. It is reassuring to notice that the new data

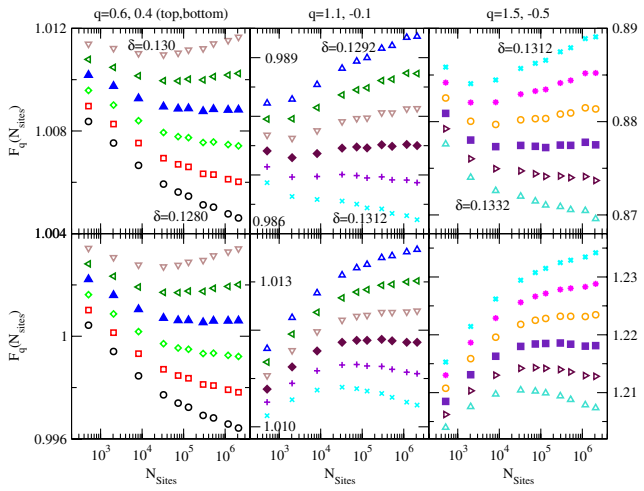

FIG. 2 (color online). Family of curves $F_q(N) = P_q N^{q-1-\delta(q-1)q}$ for $q = 0.6$, 1.1, and 1.5 (top: left, center, and right) and $q = 0.4$, -0.1, and -0.5 (bottom: left, center, and right). Each data set is labeled by a parameter δ, which increases from a minimum to a maximum value (given in the upper plots) in steps of 0.0004. The value of δ for which $F_q(N)$ is flat determines the anomalous exponent $\Delta_q = d\delta q(1-q)$. Such saturating data sets are marked with solid symbols (left: △; center:◇; right: □); typical error in the corresponding value of δ does not exceed 0.001. The change in symbols (i.e., in δ) for saturating data sets illustrates a q dependence of γ_q and thus gives direct, unprocessed evidence of nonvanishing quartic terms in Δ_q.

confirm our previous finding for b_0 but provide a much better accuracy: $b_0 = 0.1291 \pm 0.0002$. Our new result for the curvature of γ_q is $b_1 = 0.0029 \pm 0.0003$, which is clearly nonvanishing. These results are in full agreement with those obtained by a fit to $\tilde{\gamma}_q$ (see the caption to Fig. 3). We thus conclude that, although the curvature of γ_q is numerically rather small (b_1 is approximately 50 times smaller than b_0), it is nonzero: The multifractality spectrum Δ_q of the quantum Hall transition is not parabolic.

Surface exponents.—So far, a network model with torus geometry (i.e., without boundary) has been considered. Recently, it has been shown [16] that wave function fluctuations near surfaces exhibit their own multifractal spectrum with exponents Δ_q^s, defined in full analogy to Eq. (1) via

$$\langle |\psi|^{2q} \rangle_s / \langle |\psi|^2 \rangle_s^q \sim L^{-\Delta_q^s}, \tag{13}$$

with the exception that here the average $\langle \ldots \rangle_s$ is performed over the vicinity of the boundary only. In general, the surface exponents Δ_q^s are not related to their bulk counterparts in any simple manner.

To study the boundary exponents, we consider the Chalker-Coddington network of cylinder geometry, i.e., periodic in one direction and with hard-wall (full reflection) boundary conditions in the other direction. The averaging $\langle \ldots \rangle_s$ is performed over those network links that are located directly at the boundary (and includes the ensemble and the energy window averaging, as before). We parametrize the surface spectrum in analogy with the bulk case [Eqs. (2), (4), and (8)] labeling the corresponding parameters by a superscript "s." The results for γ_q^s and $\tilde{\gamma}_q^s$ are

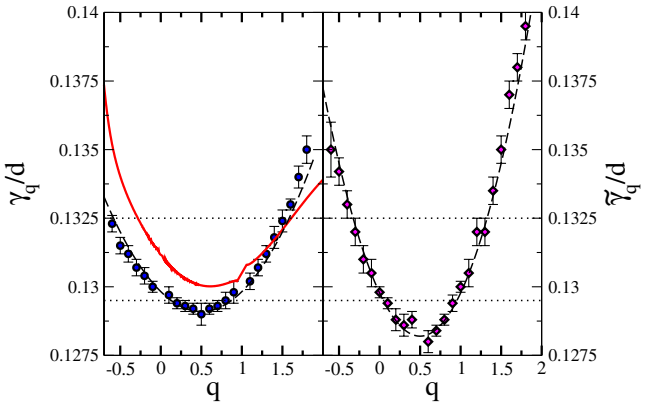

FIG. 3 (color online). The exponents $\gamma_q = \Delta_q/q(1-q)$ (○) and $\tilde{\gamma}_q = \Delta_q'/(1-2q)$ (◇) obtained from Fig. 2 and analogous analysis for other values of q. The curvature in γ_q and $\tilde{\gamma}_q$ implies that the multifractal spectrum Δ_q is not parabolic. Also shown are results of the earlier work [9] (solid line). Dotted horizontal lines indicate earlier error bars in the regime $0 \le q \le 1$. Dashed lines represent parabolic fits with $b_0 = 0.1291 \pm 0.0002$, $b_1 = 0.0029 \pm 0.0003$ (left) and $a_0 = 0.1282 \pm 0.0001$, $a_1 = 0.0063 \pm 0.0005$ (right). Combination of these data yields a rough estimate of the quartic term $b_2 = -0.001 \pm 0.001$.

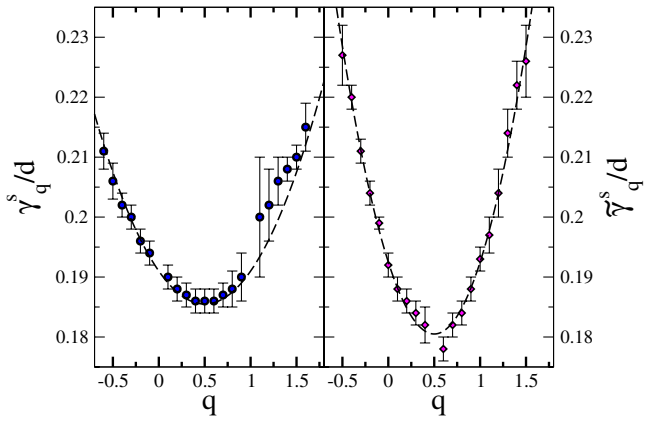

FIG. 4 (color online). The surface exponents $\gamma_q^s = \Delta_q^s/q(1-q)$. Data are presented in the form analogous to the bulk plot (Fig. 3); the curvature is even more pronounced for the surface exponents. Dashed lines indicate parabolic fits with $b_0^s = 0.1855 \pm 0.0005$, $b_1^s = 0.022 \pm 0.002$ (left) and $a_0^s = 0.1805 \pm 0.001$, $a_1^s = 0.048 \pm 0.003$ (right). The resulting estimate for b_2^s is $b_2^s = -0.008 \pm 0.01$.

shown in Fig. 4. It is seen that the nonparabolicity of the multifractality spectrum (difference of γ_q^s and $\tilde{\gamma}_q^s$ from a constant) is present at the boundary as well and is, in fact, considerably more pronounced than in the bulk. The ratio $R_q = \gamma_q^s/\gamma_q$ has a clear q dependence, with a minimum at the symmetry point $q = 1/2$, where it takes the value $R_{1/2} = 1.434 \pm 0.005$. It is also worth noticing that R_q is appreciably smaller than 2, a value naturally expected for critical theories expressed in terms of a free bosonic field.

Conclusions.—In summary, we have studied numerically the wave function statistics at the quantum Hall critical point. We have verified that the reciprocity relation (3) holds and have used it to control systematic errors related to the finite-size effects. In combination with a very large size of the statistical ensemble, this has allowed us to reach unprecedented accuracy in determination of the multifractality spectrum Δ_q, with the error bars reduced by almost an order of magnitude compared to the earlier work. The result shown in Fig. 3 reads $\Delta_q = 2q(1-q) \times [b_0 + b_1(q-1/2)^2 + b_2(q-1/2)^4 + \cdots]$, with $b_0 = 0.1291 \pm 0.0002$, $b_1 = 0.0029 \pm 0.0003$, and $b_2 = -0.001 \pm 0.001$. The obtained spectrum shows clear nonparabolicity [$b_1 \neq 0$], thus excluding a broad class of theories of the Wess-Zumino-Witten type as candidates in the conformal field theory of the quantum Hall transition. These results are corroborated by the analysis of the surface multifractality.

We thank A. Furusaki, I. A. Gruzberg, A. W. W. Ludwig, H. Obuse, and A. R. Subramaniam for useful discussions and for sharing their data prior to publication. We are also grateful to A. Tsvelik and M. R. Zirnbauer for instructive discussions. This work was supported by the Center for Functional Nanostructures of the DFG.

Note added.—Recently, we learned about an independent study by Obuse *et al.* [17], who came to the same conclusions.

*Also at Petersburg Nuclear Physics Institute, 188300 St. Petersburg, Russia.

[1] K. von Klitzing *et al.*, Phys. Rev. Lett. **45**, 494 (1980).
[2] *The Quantum Hall Effect*, edited by R. E. Prange and S. M. Girvin (Springer, New York, 1992).
[3] F. Evers and A. D. Mirlin, arXiv:0707.4378 [Rev. Mod. Phys. (to be published)].
[4] M. Zirnbauer, arXiv:hep-th/9905054v2.
[5] M. J. Bhaseen *et al.*, Nucl. Phys. **B580**, 688 (2000).
[6] A. M. Tsvelik, Phys. Rev. B **75**, 184201 (2007).
[7] While rigorously proven for a number of other Wess-Zumino-Witten models, the statement of parabolicity of Δ_q remains, strictly speaking, a plausible conjecture for the model of Ref. [4]; see also M. Bershadsky, S. Zhukov, and A. Vaintrob, Nucl. Phys. **B559**, 205 (1999).
[8] More accurately, the parabolicity may hold only for $q < q_c$; its termination at $q = q_c \equiv (2+\gamma)/2\gamma$ is related to wave function normalization; see the review [3] for details.
[9] F. Evers, A. Mildenberger, and A. D. Mirlin, Phys. Rev. B **64**, 241303(R) (2001).
[10] A. D. Mirlin, Y. V. Fyodorov, A. Mildenberger, and F. Evers, Phys. Rev. Lett. **97**, 046803 (2006).
[11] J. T. Chalker and P. D. Coddington, J. Phys. C **21**, 2665 (1988).
[12] R. Klesse and M. Metzler, Int. J. Mod. Phys. C **10**, 577 (1999).
[13] P. R. Amestoy *et al.*, Comput. Methods Appl. Mech. Eng. **184**, 501 (2000); P. R. Amestoy *et al.*, SIAM J. Matrix Anal. Appl. **23**, 15 (2001).
[14] J. W. Demmel *et al.*, SIAM J. Matrix Anal. Appl. **20**, 720 (1999).
[15] R. B. Lehoucq, D. Sorensen, and C. Yang, *ARPACK Users Guide* (SIAM, Philadelphia, 1998).
[16] A. R. Subramaniam, I. A. Gruzberg, A. W. W. Ludwig, F. Evers, A. Mildenberger, and A. D. Mirlin, Phys. Rev. Lett. **96**, 126802 (2006).
[17] H. Obuse, A. R. Subramaniam, F. Furusaki, I. A. Gruzberg, and A. W. W. Ludwig, preceding Letter, Phys. Rev. Lett. **101**, 116802 (2008).